Canadian Science Publishing
NRC Research Press journals | Publishing Services

Biochemistry and Cell Biology
Biochimie et biologie cellulaire

Ectopic expression of Miro 1 ameliorates seizure and inhibits hippocampal neurodegeneration in a mouse pilocarpine epilepsy model

Journal:	*Biochemistry and Cell Biology*
Manuscript ID	bcb-2017-0102.R3
Manuscript Type:	Article
Date Submitted by the Author:	31-Oct-2017
Complete List of Authors:	Zhang, Haifeng; The First Affiliated Hospital of Zhengzhou University, Department of Neurology Lian, Yajun; The First Affiliated Hospital of Zhengzhou University, Department of Neurology Xie, Nanchang; The First Affiliated Hospital of Zhengzhou University, Department of Neurology Zheng, Yake; The First Affiliated Hospital of Zhengzhou University, Department of Neurology
Is the invited manuscript for consideration in a Special Issue? :	N/A
Keyword:	cytochrome C, mitochondrial Rho 1, epilepsy, hippocampus, neuronal apoptosis

Ectopic expression of Miro 1 ameliorates seizure and inhibits hippocampal neurodegeneration in a mouse pilocarpine epilepsy model

Haifeng Zhang, Yajun Lian*, Nanchang Xie, Yake Zheng

Department of Neurology, The First Affiliated Hospital of Zhengzhou University, Zhengzhou 450052, People's Republic of China

*Corresponding author: Dr. Yajun Lian, Department of Neurology, The First Affiliated Hospital of Zhengzhou University, 1 East Jianshe Road, Zhengzhou 450052, People's Republic of China

Tel: +86-371-66862122

Fax: +86-371-66862121

Email: lianyajun840317@163.com

Abstract

Epilepsy is a common disease of the central nervous system. This study aims to investigate the role of mitochondrial Rho (Miro) 1 in epilepsy using a mouse model of pilocarpine-induced status epilepticus (SE). Intraperitoneal injection of pilocarpine induced epileptic seizure in mice and significantly decreased Miro 1 expression in the hippocampus. Moreover, pilocarpine treatment increased the serum levels of heat shock protein 70 (HSP70) and S100 calcium binding protein B (S100B), and led to hippocampal neuronal injury and apoptosis. The intrinsic apoptotic pathway was activated in the hippocampal neurons following pilocarpine-induced SE, as evidenced by increased levels of cleaved caspase-3 and Bax, downregulation of Bcl-2, and the release of cytochrome C from mitochondria to cytoplasm. By contrast, forced expression of Miro 1 by lateral ventricular administration of adenovirus mitigated pilocarpine-induced epileptic seizure, reduced the elevation of HSP70 and S100B, and inhibited hippocampal neuronal apoptosis by suppressing the intrinsic apoptotic pathway. In summary, our data demonstrated that ectopic expression of Miro 1 alleviated pilocarpine-induced SE and protected hippocampal neurons by inhibiting the intrinsic apoptotic pathway. These findings provide new insights in epileptic disorders and suggest a potential neuroprotective value of Miro 1 in the treatment of epilepsy.

Keywords: cytochrome C; epilepsy; hippocampus; mitochondrial Rho 1; neuronal apoptosis

Introduction

Epilepsy is one of the most common diseases of the central nervous system, with more than 50 million patients around the world and estimated 2.4 million newly diagnosed cases each year (WHO 2016). Epilepsy is a chronic brain dysfunction characterized by recurrent seizures, and temporal lobe epilepsy (TLE) is the most form of representative refractory epilepsy (Nagae et al. 2016). Hippocampal sclerosis (HS) is the most common lesion associated with TLE and it is observed in 60-75% of patients with medically intractable TLE. HS is characterized by severe neuronal loss and gliosis in hippocamal region, and the progressive volume loss in the hippocampus (Fuerst et al. 2003). Currently, the main treatment approaches for TLE are surgery and anti-epileptic drugs, but the therapeutic efficacy is not satisfactory, and some additional damages may be caused (Habibi et al. 2016; Haerian et al. 2010). Moreover, refractory epilepsy, including TLE, is resistant to a range of anti-epileptic drugs (Kwan and Brodie 2000). Therefore, it is necessary to understand the mechanism of epileptogenesis for the development of novel therapies.

Mitochondrial Rho (Miro) is a member of the Ras superfamily, and it has two isoforms: Miro 1 and Miro 2 (Fransson et al. 2003). Miro is specifically associated with mitochondria, and it was first identified in metazoans to play a critical role in the regulation of mitochondrial transport (Yamaoka and Hara-Nishimura 2014). Mitochondria are the main site of ATP production that is needed for synaptic transmission, and they also play central roles in neurotransmitter synthesis, calcium homoeostasis, redox signaling and neuronal survival (Davis and Williams 2012; Duchen 2000; Wallace et al. 2010). Mitochondrial dysfunction has been implicated in the etiology of acute seizures and chronic epilepsy (Kovacs et al. 2002). As Miro 1 is essential for axonal

mitochondrial trafficking along the microtubules (Fransson et al. 2003; Glater et al. 2006), disruption of Miro 1-dependent mitochondrial movement could result in nervous system diseases, such as Parkinson's disease and Alzheimer's disease (Iijima-Ando et al. 2012; Liu et al. 2012). A gain-of-function mutant of Miro 1 is shown to impair mitochondrial transport and cause mitochondrial aggregation (Fransson et al. 2006). In mice, loss of Miro 1 results in neural respiratory control defects, and neuron-specific Miro 1 knockout leads to upper motor neuron disease phenotypes and pathology (Nguyen et al. 2014). Although Miro 1 has been demonstrated to play an important role in the central nervous system function, its role in the pathogenesis of epileptic disorders remains elusive.

The pilocarpine-induced epilepsy model is a commonly used rodent model to reproduce human TLE characteristics because it replicates the symptoms, gene induction pattern and hippocampal neuronal loss as in TLE patients (Jefferys et al. 2016). In our preliminary study, we found that the expression of Miro 1 was decreased in the hippocampus of pilocarpine-induced epilepsy mouse model. In the present study, the implication of Miro 1 downregulation in epilepsy was investigated in a mouse model of pilocarpine-induced status epilepticus (SE). Meanwhile, the potential therapeutic effect of ectopic Miro 1 on epilepsy was assessed.

Materials and methods

Ethical statement

The procedures on the experimental animals were in line with the Guide for the Care and Use of Laboratory Animals, and the protocol was approved by the Ethics Committee of Zhengzhou University.

Animal model

The epilepsy model was established according to previously described methods (Jimenez-Mateos et al. 2015) with some modifications. Male adult C57BL/6 mice of 18-25 g (Vital River, Beijing, China) were used in this study. After being anesthetized with 10% chloral hydrate, the mice in the Model group were injected subcutaneously with scopolamine (1 mg/kg) (Sigma, St. Louis, MO, USA), followed by an intraperitoneal injection of pilocarpine (340 mg/kg) (Sigma) 30 min later to induce SE. Ninety min after pilocarpine administration, lorazepam (6 mg/kg) was injected to terminate epileptic seizures. Mice in the Sham group were anesthetized and injected with an equal volume of saline. At 4 h and 24 h after pilocarpine injection, the mice in the Sham and Model groups were sacrificed, and the hippocampal tissue samples were collected for the examination of Miro 1 expression.

To investigate the role of Miro 1 in epilepsy, mice were randomly divided into four groups: Sham, Model, negative control (NC) and Miro 1 (n=6 per group). After being anesthetized with 10% chloral hydrate, the mice in the Miro 1 group and the NC group received a lateral ventricular injecton of 2 μl (2×10^7) adenoviruses containing Miro 1 expression construct or empty NC vector (Hanbio, Shanghai, China). Twenty-four hours later, the mice in the Model, NC and Miro 1 groups were subjected to the induction of epileptic seizures as described earlier, and the sham-operated mice were injected with an equal volume of saline. Three days later, all mice were sacrificed, and their hippocampi and blood samples were collected for the subsequent analyses.

Racine scale

The severity of epileptic seizures was assessed one hour after pilocarpine injection using the Racine scale (Phelan et al. 2015). The severity was classified into five grades: Ⅰ: facial muscles twitch, including blinking, whisker shaking and chewing; Ⅱ: head nodding on top of facial and

mouth movements; Ⅲ: unilateral forelimb clonus on the top of the movements in grade Ⅱ; Ⅳ: bilateral forelimb clonus; Ⅴ: severe bilateral forelimb clonus and falling down.

RNA extraction, reverse transcription (RT) and real-time PCR

Total RNAs were extracted from the hippocampal tissues using a total RNA extraction kit (BioTeke, Beijing, China). After measurement of concentration, RNAs were reversely transcribed into cDNA by M-MLV super reverse transcriptase (BioTeke), in the presence of oligo(dT) and random primers. All instruments in this section were pre-treated with Surface RNase Erasol (TIANDZ, Beijing, China), and all reagents were RNase-free.

The cDNA was used for real-time PCR detection of Miro 1 mRNA by using 2×Power Taq PCR Master Mix (BioTeke) and SYBR Green (Solarbio, Beijing, China). The amplification procedure was set as follows: 95 ℃ for 10 min, 40 cycles of 95 ℃ for 10 s, 60 ℃ for 20 s and 72 ℃ for 30 s, and finally 4 ℃ for 5 min. The data were calculated according to the $2^{-\Delta\Delta Ct}$ method. The sequences of real-time PCR primers were shown in Table 1.

Western blot

Total cellular protein was extracted from the hippocampal tissue using RIPA lysis buffer (Wanleibio, Shenyang, Liaoning, China), and the mitochondrial protein was extracted from the hippocampal tissue with a mitochondria isolation kit (Beyotime, Haimen, Jiangsu, China) according to the manufacturer's protocol. The protein samples were denatured by 5-min boiling, separated by SDS-PAGE, and transferred onto a PVDF membrane (Millipore, Boston, MA, USA). After blocking with 5% skim milk at room temperature for 1 h, the PVDF membrane was incubated with one of the following antibodies at 4 ℃ overnight: anti-Miro 1 (1:1000; Abcam, Cambridge, UK); anti-cleaved caspase-3 (1:1000; Abcam); anti-Bax (1:2000; Proteintech, Chicago,

IL, USA); anti-Bcl-2 (1:400; Boster, Wuhan, Hubei, China); anti-cytochrome C (1:400; Boster); anti-heat shock protein 70 (HSP70) (1:500; Bioss, Beijing, China). After rinsing with TBST, the PVDF membrane was incubated with the corresponding HRP-conjugated secondary antibody at 37 ℃ for 45 min, followed by a signal exposure using the ECL reagent (Wanleibio). After removing the antibodies with stripping buffer (Wanleibio), the PVDF membrane was re-blotted with anti-β-actin (1:1000; Santa Cruz, CA, USA) or anti-voltage-dependent anion channel (VDAC) 1 (1:500; Sangon) and the secondary antibodies. β-actin served as the internal control for total cellular protein or cytosolic protein, and VDAC1 served as the internal control for mitochondrial protein.

TUNEL assay

The hippocampus was fixed with 4% paraformaldehyde (Sinopharm, Beijing, China) at room temperature overnight, dehydrated with scending concentrations of ethanol (70% for 2 h, 80% for 2 h, 90% for 2 h, and 100% for 1 h twice), permeated with xylene (Sinopharm) for 30 min, and embedded in paraffin at 60 ℃. The paraffin block was cut into sections of 5 μm. The sections were dewaxed with xylene, and rehydrated with descending concentrations of ethanol (100% for 5 min twice, 95% for 2 min, 85% for 2 min, 75% for 2 min). Thereafter, the sections were permeabilized with 0.1% Triton X-100 (Beyotime) for 8 min, blocked with 3% H_2O_2 (Sinopharm) for 10 min, and incubated with the TUNEL reagent (Roche, Basel, Switzerland) at 37 ℃ for 60 min. After washing with PBS, the sections were incubated with Converter-POD (Roche) at 37 ℃ for 30 min in the dark, and then briefly incubated with the chromogenic DAB reagent (Solarbio). Subsequently, the sections were stained with hematoxylin (Solarbio) for 3 min, soaked in 1% hydrochloric acid/ethanol for 3 s, and washed with running water for 20 min. Finally, the sections

were dehydrated with scending concentrations of ethanol (75% for 2 min, 85% for 2 min, 95% for 2 min, and 100% for 10 min twice) and xylene (10 min twice), mounted with gum, and photographed by microscopy (Olympus, Tokyo, Japan). The number of TUNEL-positive cells and total cells on each coronal section was counted by two pathologists without knowing the group setting, and the obtained data were further averaged. The apoptosis rate = TUNEL-positve cell number/ total cell number x 100%.

Nissl staining

The hippocampal tissue was processed into paraffin sections according to the previously described method, followed by deparaffinization and rehydration. After removing the residual liquid, the sections were stained with 0.5% cresyl violet (Sinopharm) for 10 min, soaked in 0.25% acetic acid/ethanol (Kermel, Tianjin, China), and dehydrated with 100% ethanol for 5 min twice and then with xylene for 10 min twice. Finally, the sections were mounted gum, and photographed with a microscope (Olympus).

Immunohistochemistry

The hippocampal sections were dewaxed, rehydrated and subjected to heated antigen retrieval. After blocking with 3% H_2O_2 for 15 min and then with goat serum (Solarbio) for 15 min, the sections were incubated with an antibody against Miro 1 (1:200; Abcam) at 4 ℃ overnight, and then incubated with biotin-labeled goat anti-mouse IgG (1:200; Beyotime) at 37 ℃ for 30 min. Subsequently, the sections were incubated with streptavidin-HRP (Beyotime) at 37 ℃ for 30 min in the dark, developed with DAB (Solarbio), and counterstained with hematoxylin (Solarbio). Finally, the sections were dehydrated, mounted, and observed under microscope at 400× magnification.

Enzyme-linked immunosorbent assay (ELISA)

The levels of HSP70 and S100 calcium binding protein B (S100B) in the serum were determined with the HSP70 ELISA kit and the S100B ELISA kit (USCN, Wuhan, Hubei, China), respectively, according to the manufacturer's instructions.

HSP70 standards (50, 25, 12.5, 6.25, 3.12, 1.56 and 0.78 ng/ml) were mixed with Detection A solution (1:100, diluted with water), and incubated at 37 ℃ for 1 h. After washing thrice with the washing buffer, the standards were incubated with Detection B solution (1:100, diluted with water) at 37 ℃ for 30 min, washed 5 times, and reacted with TMB substrate at 37 ℃ in the dark. Later on, the reaction was terminated by adding the termination buffer, and the optical density (OD) was detected at 450 nm. The standard curve of the HSP70 was drawn based on the OD_{450} of HSP70 standards. The OD_{450} of each serum sample was measured in the same way, and the concentration of HSP70 was calculated according to the standard curve.

S100B standard curve was drawn using S100B standards (1000, 500, 250, 125, 62.5, 31.2 and 15.6 pg/ml) following the same procedures as for HSP70. The S100B concentration in the serum was detected and calculated based on the S100B standard curve.

Statistical analysis

The data in this study were presented as mean ± SD of six individuals in each group. The Racine scores were analyzed by Wilcoxon signed rank test. The differences in Miro 1 expression between the Sham and the Model groups at 4 h and 24 h were analyzed by two-way ANOVA test, and differences between the Sham, Model, NC and Miro 1 groups were analyzed by one-way ANOVA test with post hoc Bonferroni's multiple comparisons. $P<0.05$ was considered statistically significant (*$p<0.05$, **$p<0.01$, ***$p<0.001$).

Results

Expression of Miro 1 was decreased in mouse hippocampus after pilocarpine-induced SE

Epilepsy was induced in mice by intraperitoneal injection of pilocarpine, and the expression levels of Miro 1 in the hippocampus were detected by real-time PCR and western blot 4 h and 24 h after pilocarpine injection. The results showed that the mRNA level of Miro 1 was decreased by 54% ($P<0.001$) and 61% ($P<0.001$) at post-induction 4 h and 24 h, respectively (Fig. 1A). Consistently, Miro 1 protein was decreased by 79% ($P<0.001$) and 85% ($P<0.001$), respectively, at 4 h and 24 h after pilocarpine administration (Fig. 1B). These results suggest that downregulation of Miro 1 may be associated with pilocarpine-induced SE.

Ectopic expression of Miro 1 alleviated pilocarpine-induced epileptic seizure and reversed the upregulation of TLE markers

To investigate the implication of Miro 1 downregulation in pilocarpine-induced epilepsy, adenovirus containing Miro 1 expression construct was injected into the lateral ventricle one day before the induction of epilepsy. One hour after pilocarpine injection, the Racine scale was used to assess the severity of epilepsy seizures in the four groups of mice. As shown in Fig. 2A, pilocarpine induced epilepsy seizure in mice ($P=0.0335$), and adenovirus-mediated expression of Miro 1 significantly alleviated seizure severity ($P=0.0477$) as compared with the NC group. Moreover, two epilepsy markers, HSP70 and S100B (Chang et al. 2012; Yang et al. 2008) were examined after pilocarpine-induced SE. As shown in Fig. 2B and C, the levels of HSP70 in the hippocampus and the serum increased 4.05-fold ($P<0.001$) and 3.99-fold ($P<0.001$), respectively, three days after pilocarpine injection. By contrast, ectopic expression of Miro 1 decreased hippocampal and serum levels of HSP70 by 57% ($P<0.001$) and 40% ($P<0.01$), respectively (Fig. 2B

and C). Similarly, delivery of Miro 1 expression adenovirus to the lateral ventricle attenuated the elevation of serum S100B following pilocarpine-induced SE (Fig. 2D). In addition, immunoblotting and immunohistochemical results revealed that the Miro 1 expression was reduced by 82% ($P<0.001$) three days after pilocarpine treatment, whereas adenovirus-mediated expression of Miro 1 restored Miro 1 expression in the hippocampus (Fig. 2E).

Forced expression of Miro 1 reduced pilocarpine-induced hippocampal neuronal injury and apoptosis

Since neuronal dysfunction and injury always exists in epilepsy, Nissl staining and TUNEL assay were performed to detect hippocampal neuronal injury and apoptosis three days after pilocarpine-induced SE. The Nissl staining result showed that pilocarpine injection caused prominent neuronal injury in the hippocampus, and the survived neuron number was decreased by 88% ($P<0.001$), however, it was increased 4.45-fold ($P<0.001$) by ectopic Miro 1 expression (Fig. 3A-B). The TUNEL results showed that the apoptosis rate in the hippocampus was elevated 77.79-fold ($P<0.001$), but reduced by 50% ($P<0.001$) after Miro 1 ectopic expression (Fig. 3C-D). In addition, three important apoptotic executors, cleaved caspase-3, Bax, and Bcl-2, were detected by western blotting. The results showed that pilocarpine treatment led to 3.17-fold elevation of cleaved caspase-3 ($P<0.001$) and 3.34-fold elevation of Bax ($P<0.001$) in the hippocampal tissue, and it also reduced the expression of Bcl-2 by 55% ($P<0.001$). Compared with the NC group, forced expression of Miro 1 reduced levels of cleaved caspase-3 and Bax by 53% ($P<0.001$) and 36% ($P<0.05$), respectively, and increased the expression of Bcl-2 by 1.4-fold ($P<0.01$) (Fig. 4A and B). These results demonstrated that Miro 1 inhibited hippocampal neuronal apoptosis in mice after pilocarpine-induced SE.

Miro 1 inhibited pilocarpine-induced release of cytochrome C in hippocampal neurons

Cell apoptosis can be classified into the extrinsic pathway or the intrinsic pathway, wherein the former is activated by dead receptor and the latter is mediated by the release of cytochrome C from mitochondria (Sarvothaman et al. 2015). As Miro 1 is associated with mitochondrial function, we speculated that the neuronal apoptosis in the epileptic mice may be initiated by the intrinsic pathway. Thus, the subcellular localization of cytochrome C, the key mediator of intrinsic apoptotic pathway, was measured. The immunoblotting results showed that the content of cytochrome C in the cytoplasm was increased 2.56-fold ($P<0.001$) and the content in the mitochondria was decreased by 65% ($P<0.001$) three days after pilocarpine treatment (Fig. 4C and D). However, the expression of exogenous Miro 1 downregulated the level of cytosolic cytochrome C by 29% ($P<0.05$) and elevated the content of mitochondrial cytochrome C by 1.68-fold ($P<0.05$) compared with the NC group (Fig. 4C and D). These results demonstrated that forced expression of Miro 1 inhibited the release of cytochrome C from mitochondria into cytoplasm, thus blocked the intrinsic apoptotic pathway in the hippocampal neurons after pilocarpine-induced SE.

Discussion

In mammalian and human neurons, mitochondrial transport along axons and dendrites is essential for ensuring ATP availability during the energetically-demanding process at the synapses (Harris et al. 2012). Disruption of mitochondrial function, transport or distribution can lead to nervous system disorders, such as epilepsy. Axonal mitochondrial transport relies on the microtubule-based kinesin and dynein (Sheng 2014), and Miro 1 is associated with both classes of motor proteins. Kinesin binds cargo via its light chains, the kinesin adaptor Milton recruits kinesin

heavy chain to the mitochondrion and interacts directly with Miro 1 (Glater et al. 2006). It has been reported that Miro 1 knockout mice were cyanotic, having unexpanded lungs and died very shortly after birth (Nguyen et al. 2014). The mutant yeast strain of *gem1*, encoding a homologue of Miro in *S. cerevisiae*, grew significantly slower than the wild-type strain and exhibited distorted mitochondrial morphology and defective mitochondrial distribution (Frederick et al. 2004). Moreover, knockdown of *miro* homologous genes in zebrafish resulted in posterior body-axis elongation defects and a smaller head, and ultimately embryonic lethality (Hollister et al. 2016).

In our study, Miro 1 was decreased in the hippocampus of mice with pilocarpine-induced SE. At the same time, pilocarpine led to elevation of two epilepsy markers, HSP70 and S100B, as well as neuronal injury in the hippocampus. Restoration of Miro 1, however, attenuated the epileptic seizure, reduced the ascents of HSP70 and S100B, and suppressed hippocampal neuronal apoptosis in pilocarpine-treated mice. These results suggest that Miro 1 plays a critical role in pilocarpine-induced epilepsy.

It is well known that epilepsy is associated with mitochondrial dysfunction (Zsurka and Kunz 2015), and Miro 1 plays a crucial role in mitochondrial transport and function. Thus, loss of Miro 1 may lead to mitochondrial dysfunction and epileptogenesis. In addition to the defects in mitochondrial morphology and distribution, downregulation of Miro 1 was found associated with an increased level of Bax, a decreased level of Bcl-2 and translocation of cytochrome C from mitochondria to cytoplasm following pilocarpine-induced SE. It is known that allosterically activated Bax/Bak causes the permeabilization of mitochondrial outer membrane and the release of cytochrome C, for the initiation of intrinsic apoptosis, whereas the allosteric activation of Bax/Bak could be inhibited by Bcl-2/Bcl-XL (Kvansakul and Hinds 2015; Sarvothaman et al. 2015).

In our study, pilocarpine-induced upregulation of Bax, downregulation of Bcl-2 and mitochondrial release of cytochrome C were abolished by ectopic expression of Miro 1. Thus, we conclude that Miro 1 inhibits epilepsy-associated release of cytochrome C and activation of the intrinsic apoptosis pathway by modulating the expression of Bcl-2 family members.

TLE is the most common refractory epilepsy with complex and unclear etiology. Recently, increasing evidences have implicated the dysfunction and deregulated distribution of mitochondria in the pathogenesis of TLE (Nguyen et al. 2014). In this study, forced expression of Miro 1 alleviated epileptic seizure and inhibited hippocampal neuronal apoptosis by suppressing the intrinsic apoptosis pathway in pilocarpine-induced SE mice. As the rodent pilocarpine model is a well-recognized TLE model, our findings may provide new insights in the anticonvulsant and neuroprotective properties of Miro 1 in TLE, and this may have clinical significance for the treatment of TLE. Seizures are known to damage the hippocampus, particularly prolonged seizures and SE, and neuronal loss is the primary charateristic. To protect the hippocampal neurons is important for the intervention and prevention of epilepsy (Thom et al. 2005). Our data demonstrated that the hippocampal neuronal injury and apoptosis after SE were significantly mitigated by the ectopic expression of Miro 1.

However, our study demonstrated a beneficial effect of ectopic Miro 1 against acute epileptic seizure, whether Miro 1 exhibits a therapeutic effect in a long run demands further study.

Conclusion

Ectopic expression of Miro 1 ameliorated pilcarpine-induced SE, and exerted hippocampal neuroprotection by inhibiting intrinsic apoptosis in a mouse epilepsy model. Our findings may provide new insights in the pathological mechanism of TLE, and may be of clinical significant for

296 the treatment of TLE.

Acknowledgment

This study was supported by grants from the National Natural Science Foundation of China (No. 81701271, 81771397 and 81701295).

Disclosure of competing interests

The authors declare that there is no conflict of interest.

References

Chang, C.C., Lui, C.C., Lee, C.C., Chen, S.D., Chang, W.N., Lu, C.H., Chen, N.C., Chang, A.Y., Chan, S.H., and Chuang, Y.C. 2012. Clinical significance of serological biomarkers and neuropsychological performances in patients with temporal lobe epilepsy. BMC Neurol **12**: 15.

Davis, R.E., and Williams, M. 2012. Mitochondrial function and dysfunction: an update. J Pharmacol Exp Ther **342**(3): 598-607.

Duchen, M.R. 2000. Mitochondria and calcium: from cell signalling to cell death. J Physiol **529 Pt 1**: 57-68.

Fransson, A., Ruusala, A., and Aspenstrom, P. 2003. Atypical Rho GTPases have roles in mitochondrial homeostasis and apoptosis. J Biol Chem **278**(8): 6495-6502.

Fransson, S., Ruusala, A., and Aspenstrom, P. 2006. The atypical Rho GTPases Miro-1 and Miro-2 have essential roles in mitochondrial trafficking. Biochem Biophys Res Commun **344**(2): 500-510.

Frederick, R.L., McCaffery, J.M., Cunningham, K.W., Okamoto, K., and Shaw, J.M. 2004. Yeast Miro GTPase, Gem1p, regulates mitochondrial morphology via a novel pathway. J Cell Biol **167**(1): 87-98.

Fuerst, D., Shah, J., Shah, A., and Watson, C. 2003. Hippocampal sclerosis is a progressive disorder: a longitudinal volumetric MRI study. Ann Neurol **53**(3): 413-416.

Glater, E.E., Megeath, L.J., Stowers, R.S., and Schwarz, T.L. 2006. Axonal transport of mitochondria requires milton to recruit kinesin heavy chain and is light chain independent. J Cell Biol **173**(4): 545-557.

Habibi, M., Hart, F., and Bainbridge, J. 2016. The Impact of Psychoactive Drugs on Seizures and Antiepileptic Drugs. Curr Neurol Neurosci Rep **16**(8): 71.

Haerian, B.S., Roslan, H., Raymond, A.A., Tan, C.T., Lim, K.S., Zulkifli, S.Z., Mohamed, E.H., Tan, H.J., and Mohamed, Z. 2010. ABCB1 C3435T polymorphism and the risk of resistance to antiepileptic drugs in epilepsy: a systematic review and meta-analysis. Seizure **19**(6): 339-346.

Harris, J.J., Jolivet, R., and Attwell, D. 2012. Synaptic energy use and supply. Neuron **75**(5): 762-777.

Hollister, B.M., Oonk, K.A., Weiser, D.C., and Walsh, S. 2016. Characterization of the three zebrafish orthologs of the mitochondrial GTPase Miro/Rhot. Comp Biochem Physiol B Biochem Mol Biol **191**: 126-134.

Iijima-Ando, K., Sekiya, M., Maruko-Otake, A., Ohtake, Y., Suzuki, E., Lu, B., and Iijima, K.M. 2012. Loss of axonal mitochondria promotes tau-mediated neurodegeneration and Alzheimer's disease-related tau phosphorylation via PAR-1. PLoS Genet **8**(8): e1002918.

Jefferys, J., Steinhauser, C., and Bedner, P. 2016. Chemically-induced TLE models: Topical application. J Neurosci Methods **260**: 53-61.

Jimenez-Mateos, E.M., Engel, T., Merino-Serrais, P., Fernaud-Espinosa, I., Rodriguez-Alvarez, N., Reynolds, J., Reschke, C.R., Conroy, R.M., McKiernan, R.C., deFelipe, J., and Henshall, D.C. 2015. Antagomirs targeting microRNA-134 increase hippocampal pyramidal neuron spine volume in vivo and protect against pilocarpine-induced status epilepticus. Brain Struct Funct **220**(4): 2387-2399.

Kovacs, R., Schuchmann, S., Gabriel, S., Kann, O., Kardos, J., and Heinemann, U. 2002. Free radical-mediated cell damage after experimental status epilepticus in hippocampal slice cultures. J Neurophysiol **88**(6): 2909-2918.

Kvansakul, M., and Hinds, M.G. 2015. The Bcl-2 family: structures, interactions and targets for

drug discovery. Apoptosis **20**(2): 136-150.

Kwan, P., and Brodie, M.J. 2000. Early identification of refractory epilepsy. N Engl J Med **342**(5): 314-319.

Liu, S., Sawada, T., Lee, S., Yu, W., Silverio, G., Alapatt, P., Millan, I., Shen, A., Saxton, W., Kanao, T., Takahashi, R., Hattori, N., Imai, Y., and Lu, B. 2012. Parkinson's disease-associated kinase PINK1 regulates Miro protein level and axonal transport of mitochondria. PLoS Genet **8**(3): e1002537.

Nagae, L.M., Lall, N., Dahmoush, H., Nyberg, E., Mirsky, D., Drees, C., and Honce, J.M. 2016. Diagnostic, treatment, and surgical imaging in epilepsy. Clin Imaging **40**(4): 624-636.

Nguyen, T.T., Oh, S.S., Weaver, D., Lewandowska, A., Maxfield, D., Schuler, M.H., Smith, N.K., Macfarlane, J., Saunders, G., Palmer, C.A., Debattisti, V., Koshiba, T., Pulst, S., Feldman, E.L., Hajnoczky, G., and Shaw, J.M. 2014. Loss of Miro1-directed mitochondrial movement results in a novel murine model for neuron disease. Proc Natl Acad Sci U S A **111**(35): E3631-3640.

Phelan, K.D., Shwe, U.T., Williams, D.K., Greenfield, L.J., and Zheng, F. 2015. Pilocarpine-induced status epilepticus in mice: A comparison of spectral analysis of electroencephalogram and behavioral grading using the Racine scale. Epilepsy Res **117**: 90-96.

Sarvothaman, S., Undi, R.B., Pasupuleti, S.R., Gutti, U., and Gutti, R.K. 2015. Apoptosis: role in myeloid cell development. Blood Res **50**(2): 73-79.

Sheng, Z.H. 2014. Mitochondrial trafficking and anchoring in neurons: New insight and implications. J Cell Biol **204**(7): 1087-1098.

Thom, M., Zhou, J., Martinian, L., and Sisodiya, S. 2005. Quantitative post-mortem study of the hippocampus in chronic epilepsy: seizures do not inevitably cause neuronal loss. Brain **128**(Pt 6): 1344-1357.

368 Wallace, D.C., Fan, W., and Procaccio, V. 2010. Mitochondrial energetics and therapeutics. Annu
369 Rev Pathol **5**: 297-348.
370 WHO. 2016. Epilepsy fact sheet.
371 Yamaoka, S., and Hara-Nishimura, I. 2014. The mitochondrial Ras-related GTPase Miro: views
372 from inside and outside the metazoan kingdom. Front Plant Sci **5**: 350.
373 Yang, T., Hsu, C., Liao, W., and Chuang, J.S. 2008. Heat shock protein 70 expression in epilepsy
374 suggests stress rather than protection. Acta Neuropathol **115**(2): 219-230.
375 Zsurka, G., and Kunz, W.S. 2015. Mitochondrial dysfunction and seizures: the neuronal energy
376 crisis. Lancet Neurol **14**(9): 956-966.
377
378

Figure legends

Fig. 1 Miro 1 was decreased in mouse hippocampus after pilocarpine-induced SE

(A) The mRNA level of Miro 1 in the hippocampus of pilocarpine-treated mice was detected by real-time PCR 4 h and 24 h after pilocarpine injection. (B) The protein level of Miro 1 in mouse hippocampus was detected by western blot in 4 h and 24 h after induction of epilepsy. n=6 each group; the data were analyzed by two-way ANOVA test; **P<0.05, **P<0.01, ***P<0.001*; Miro 1, mitochondrial Rho 1.

Fig. 2 Ectopic expression of Miro 1 inhibited pilocarpine-induced epileptic seizure and attenuated the upregulation of epileptic markers

(A) The Racine scale was employed to assess the severity of epileptic seizure of mice one hour after pilocarpine injection. (B) The expression level of HSP70 in the hippocampus was detected by western blot 3 days after pilocarpine administration. (C) The expression level of HSP70 in serum was detected by ELISA 3 days after pilocarpine-induced SE. (D) The expression level of S100B in the serum was detected by ELISA 3 days after pilocarpine-induced SE. (E) The expression level of Miro 1 in the hippocampus tissue 3 days after pilocarpine administration was detected by western blotting. (F) Immunohistochemistry was performed to detect the expression level of Miro 1 in the hippocampus (scale bar represents 50 μm). n=6 each group; the data of Racine scores were analyzed by Wilcoxon signed rank test, and the data of ELISA and western blot were analyzed by one-way ANOVA test with post hoc Bonferroni's multiple comparisons; **P<0.05, **P<0.01, ***P<0.001*; Miro 1, mitochondrial Rho 1; HSP70, heat shock protein 70; S100B, S100 calcium binding protein B; ELISA, enzyme-linked immunosorbent assay.

Fig. 3 Forced expression of Miro 1 reduced hippocampal neuronal injury and apoptosis after

pilocarpine-induced SE

(A) Nissl staining was performed to detect hippocampal neuronal injury 3 days after pilocarpine-induced SE (scale bar in images of 40x magnification represents 500 μm, scale bar in images of 200x magnification represents 100 μm, scale bar in images of 400x magnification represents 50 μm; the injured neurons were indicated with arrows). (B) The survived neuron numbers in the hippocampus were counted in the 400x images of (A). (C) TUNEL assay was performed to detect hippocampal neuronal apoptosis 3 days after pilocarpine injection (scale bar in images of 400x magnification represents 50 μm, scale bar in images of 600x magnification represented 50 μm; the TUNEL-positive neurons were indicated with arrows). (D) The TUNEL-positive cell percentage in the hippocampus was calculated. n=6 each group; the data were analyzed by one-way ANOVA test with post hoc Bonferroni's multiple comparisons; **P<0.05, **P<0.01, ***P<0.001*; Miro 1, mitochondrial Rho 1.

Fig. 4 Miro 1 inhibited pilocarpine-induced intrinsic apoptosis in the hippocampal neurons

(A) and (B) The levels of cleaved caspase-3, Bax and Bcl-2 in the hippocampus were detected by western blot 3 days after pilocarpine-induced SE. (C) and (D) The levels of cytochrome C in the cytoplasm and mitochondria of hippocampal neurons were detected by western blot 3 days after pilocarpine administration. n=6 in each group; the data were analyzed by two-way ANOVA test; **P<0.05, **P<0.01, ***P<0.001*; Miro 1, mitochondrial Rho 1.

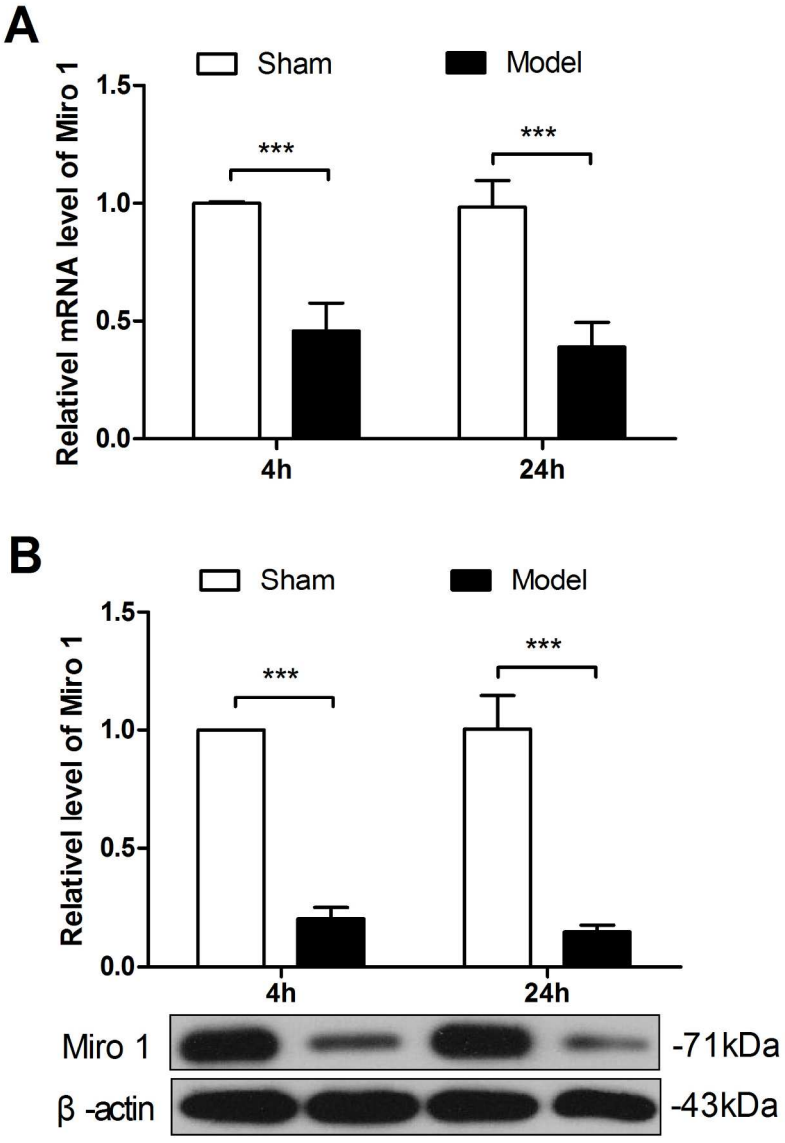

figure 1

164x235mm (300 x 300 DPI)

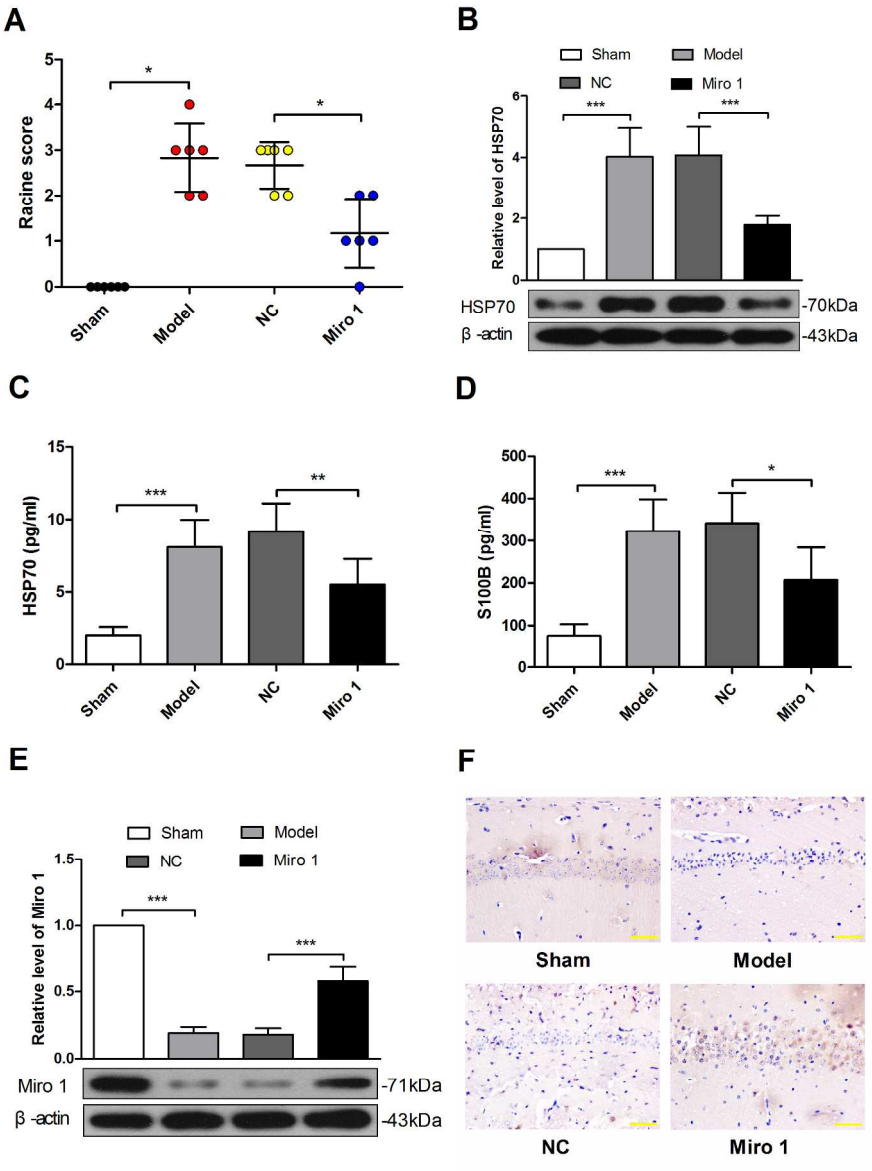

figure 2

202x267mm (300 x 300 DPI)

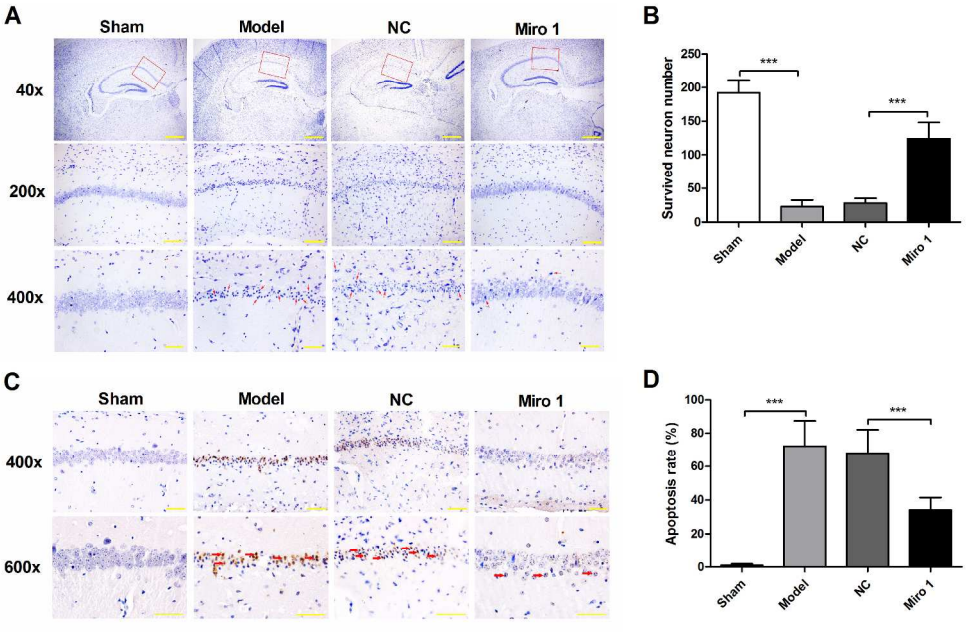

figure 3

286x187mm (300 x 300 DPI)

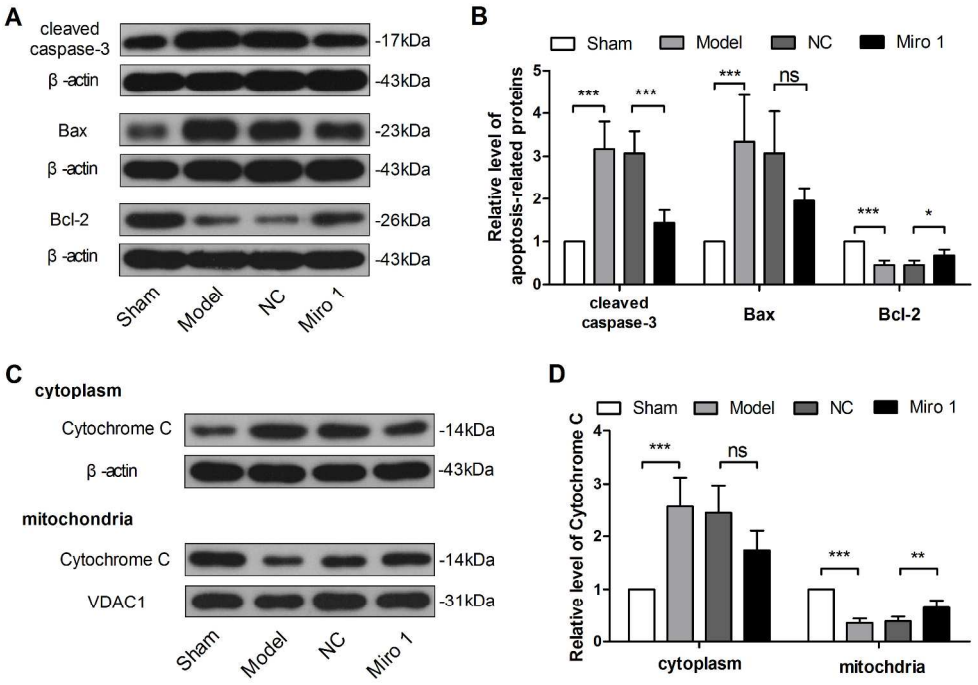

figure 4

280x201mm (300 x 300 DPI)

Tables

Table 1. The information of real-time PCR primers used in this study.

Name	Sequence	Length	Tm	Length of amplicon	Gene ID
Miro 1 F	5’-CGACGATTTGGTTATGACGATG-3’	22nt	60.6℃	173bp	NM_021536.7
Miro 1 R	5’-AGTTCATCAGGCGACAAAGCAC-3’	22nt	61.8℃		
β-actin F	5’-CTGTGCCCATCTACGAGGGCTAT-3’	23nt	64.5℃	155bp	NM_007393.5
β-actin R	5’-TTTGATGTCACGCACGATTTCC-3’	23nt	63.2℃		

Abbreviation: Miro 1: Mitochondrial Rho 1; F: forward; R: reverse; nt: nucleotide; Tm: temperature of melting; bp: base pair